Glucose Electrooxidation for Biofuel Cell Applications

I. Ivanov,[a] T. R. Vidaković,[b,*] and K. Sundmacher[a,b]

[a]Max-Planck-Institute for Dynamics of Complex Technical Systems, Sandtorstrasse 1, D-39106 Magdeburg, Germany

[b]Otto-von-Guericke-University Magdeburg, Process Systems Engineering, Universitätsplatz 2, D-39106 Magdeburg, Germany

Original scientific paper
Received: July 16, 2008
Accepted: November 24, 2008

The kinetics of glucose electrooxidation on different catalysts has been studied at physiological conditions (pH 7 and 37 ^{0}C). Electrochemically activated rough gold, rough gold modified with a self-assembled monolayer (SAM) of cystamine and an enzymatic electrode based on a charge transfer complex (CTC) and glucose oxidase (GOx) have been tested. The influence of glucose concentration, electrode rotation rate and presence of oxygen has been investigated and the stability of the different catalysts has been evaluated. All parameters have been discussed in the context of the potential application of these catalysts in an implantable glucose/O_2 biofuel cell. Rough gold exhibits high activity with very low overpotential for glucose oxidation but its extreme instability and low oxygen tolerance make it inappropriate as potential anode in a biofuel cell. The CTC enzymatic electrode on the other side shows high activity for glucose oxidation, reasonably low overpotential and relatively high stability.

Key words:
Glucose oxidation, Gold, SAM, Charge Transfer Complex, Glucose oxidase

Introduction

The electrooxidation of glucose has been extensively studied due to the increasing interest in the development of glucose biosensors and glucose biofuel cells.[1–3] As catalysts enzymes (biocatalysts)[1,2] as well as conventional metal catalysts[3] have been tested. The advantages of biocatalysts are high selectivity, high turnover number and the ability to catalyze different reactions at physiological temperature and pH, tolerating fuel and oxidant in the same solution. Additionally, enzymes are renewable and can be produced using low-cost fermentation techniques.[4] All these features enable simple fuel cell design (e.g. membraneless cell construction). However, enzymatic catalysts have several drawbacks like low long-term stability and efficient regeneration of the enzyme after the catalytic reaction (i.e. coupling of an enzymatic catalyst with electron conductive surface, which brings back the enzyme into its oxidized form). Alternative are metal catalysts, which can oxidize glucose efficiently, but they suffer from lower sensitivity and long-term stability is also an open issue. Also, the cost of metal catalysts is usually higher.

Among metal catalysts, gold has received perhaps the most attention.[5–15] The activity of gold for glucose oxidation is influenced by composition and pH value of the electrolyte,[5,6] surface structure,[7–11] surface preconditioning,[8–10] temperature[10] and surface modification.[10] Gold exhibits high catalytic activity but only in neutral and alkaline media due to the fact that the glucose oxidation mechanism involves $AuOH_{ads}$ layer (a precursor of the gold oxide layer) formation,[7] which is more favorable at higher pH values. The formation of $AuOH_{ads}$ layer is a surface sensitive reaction, which means that glucose oxidation on different gold single crystal surfaces proceeds with different reaction rates.[7] Different means of surface preconditioning have been tested in literature e.g. mechanical polishing[8] and chemical treatment (amalgamation)[8] or electrochemical preconditioning in different potential windows.[10] Gold, subjected to mechanical polishing had lower activity than gold subjected to amalgamation (produce very rough surface) and the latter was employed as a glucose sensor with an improved performance.[9] The influence of the applied potential window was discussed in our recent work.[10] It was shown that the potential cycling in an extended potential window (between hydrogen and oxygen evolution) can regenerate gold electrocatalytic activity, but it leads to a decrease of real surface due to some kind of surface "self-annealing" process. Temperature has significant influence on rough gold activity, as shown in our recent publication.[10] It accelerates the transformation of "active" (exhibits high activity for glucose oxidation) into "inactive"

*Corresponding author.
E-mail address: vidakovi@mpi-magdeburg.mpg.de

(exhibits low activity for glucose oxidation) surface. Surface modification with foreign ad-atoms[13–15] and a self-assembled monolayer (SAM)[10] have been reported. Gold modified by Ag ad-atoms exhibits a negative shift in the oxidation onset and improved stability compared to bare gold.[13,14] Gold modified by SAM was shown to have catalytic activity for oxygen reduction[16] and recently for glucose oxidation.[10]

Enzymatic electrodes for glucose oxidation employ mainly enzyme glucose oxidase (GOx) as a biocatalyst. There are a number of other enzymes which can be used (see e.g. an overview of different enzymatic catalysts for glucose oxidation[17]), but GOx is favored due to high turnover number for glucose oxidation, high sensitivity and stability. The drawback is the difficulty in establishing direct electron transfer between the enzyme and the electrode surface i.e. the enzyme regeneration. To overcome this problem several approaches have been suggested in literature. It is worth to mention the approach first reported by Heller's group[18] and later adopted by several other groups,[19–21] which is based on osmium based redox polymers and shows rapid electron transfer and low overpotential for glucose oxidation. The mechanism of electron transfer between the enzyme and the polymer is described as mediated and it is determined by the reversible potential of Os redox pair. The drawback of this method is long and complicated polymer synthesis and relatively low long-term stability. Another approach that deserves special attention is the one based on conductive organic salts (charge transfer complexes, CTC) first reported by Čenas and Kulys[22] and later adopted by several other groups.[24–27] The most common CTC used in such architectures is the complex between tetrathiafulvalene (TTF) and tetracyanoquinodimethane (TCNQ) and its applications in biosensing devices have been reviewed recently.[28] Enzymatic electrodes based on CTC exhibit low overpotentials, high current density for glucose oxidation, excellent long-term stability (e.g. 40 % residual response after 100 days of continuous operation[26]) and relatively simple preparation method. Regarding the electron transfer mechanism there is still some controversy in the literature. Some authors suggested a mediated electron transfer (MET),[22–24] while other suggested direct electron transfer (DET)[25–27] mechanism.

In the present work, the kinetics of glucose oxidation on different catalysts (two metal catalysts and one biocatalyst) is studied. All studies were performed at physiological conditions (neutral pH and 37 ^{0}C) which were chosen with respect to the potential use of these catalysts in a direct glucose fuel cell for *in vivo* application in the human body. As metal catalysts, rough gold and gold modified by SAM have been chosen, since our recent study[10] showed that these two surfaces have high activity for glucose oxidation. As a biocatalyst enzymatic electrode based on GOx and CTC was used. The influence of glucose concentration, rotation rate and oxygen was studied. Also, the loss of activity during polarization at constant potential was evaluated. Some kinetic parameters have been determined and the overall performance has been discussed in the context of the potential application of such electrodes in a direct glucose biofuel cell.

Experimental

Materials

Polycrystalline gold (99.999 %) was supplied by Aldrich and cut into discs (9 mm diameter, 2 mm thickness). For pyrrole electropolymerisation, stainless steel discs (11 mm diameter, 1 mm thickness) were used. Both types of discs were mounted in a sample holder for rotating disc electrode (Radiometer Analytical) with an opening of 6 mm (0.28 cm^2 working area) for all electrochemical tests (with an exception of the electropolymerisation experiments, where an opening of 8 mm and 0.5 cm^2 working area was used). Glucose oxidase (EC 1.1.3.4, GOx) from *Aspergillus niger* was supplied by Fluka. All other chemicals including glucose, cystamine, TTF, TCNQ and polyvinyl sulfate potassium salt (PVS) as well as solvents tetrahydrofuran (THF) and acetonitrile (ACN) were of analytical reagent grade and purchased from Aldrich or Fluka. Ultrapure water from Millipore® was used in all experiments.

Scanning electron microscopy (SEM)

The morphology of the electrode surfaces were investigated with a scanning electron microscopy (SEM) (DSM 942, Zeiss).

Electrochemical experiments

Electrochemical experiments were carried out in a conventional double-jacketed Pyrex electrochemical cell (Radiometer Analytical). The rotating discs were used as working electrodes, platinum wire as a counter electrode, and a saturated calomel electrode (SCE) was used as a reference electrode. All potentials in this paper were cited versus SCE (0.24 V *vs*. standard hydrogen electrode (SHE)). The experimental solutions were thoroughly deoxygenated with pure nitrogen with the exception of tests in the presence of oxygen. Electrochemical experiments were performed by a computer controlled

potentiostat PGSTAT302 (Eco Chemie/Autolab, Netherlands).

Gold pretreatment and modification

The polycrystalline gold surface was subjected to different pre-treatments before self-assembly of cystamine and tests for glucose oxidation. After electrochemical polishing[29] and flame annealing, the surface was roughened by amalgamation, which consisted of contacting the electrode with liquid mercury (usually for 10 s), followed by dissolving of the formed amalgam layer in concentrated nitric acid.

For the tests with bare gold, freshly roughened gold was used and electrochemical (EC) activation was applied before every electrochemical experiment. It consisted of 5 potential cycles (at 200 mV s^{-1}) between –1 V and 1.3 V in 0.1 M phosphate buffer solution (pH 7.2).

Modification with cystamine was performed by soaking the freshly roughened gold (not subjected to electrochemical activation) in 0.04 M cystamine solution for 2 h and rinsing the electrode thoroughly with water. Schematic presentations of the rough gold surface and the rough gold modified with cystamine are shown in Fig. 1a, b.

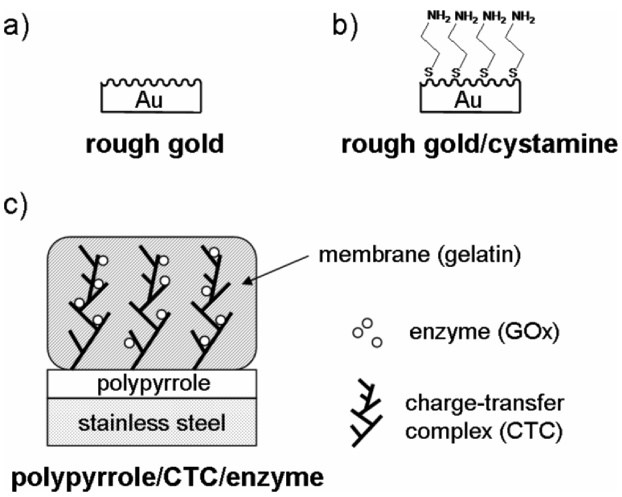

Fig. 1 – *Schematic presentation of the layer structure of the different electrode surfaces used for glucose oxidation*

Electrochemical characterization in 0.1 M phosphate buffer solution and in potential window between –0.6 V and 0.5 V was performed between the above mentioned steps.

Enzymatic modification

For fabrication of the enzymatic electrode, a modified version of the procedure described by Kahn *et al*.[26] was used. First, a polymer film was formed on stainless steel electrode rotating at 400 rpm (rounds per minute). The electropolymerisation was done anodically at a current density of 2.4 mA cm^{-2} until a charge of 8.64 C cm^{-2} passed, in a water solution containing typically 2 mM (monomer molecular weight) PVS and 15 mM pyrrole. No attempts to exclude oxygen from the system were made.

The second step was the growth of the CTC on the polymer surface, which proceeded in two steps. First, the TCNQ dissolved in THF was applied to the polymer surface and left to dry. Successively, TTF dissolved in ACN was cast onto the polymer film. In both steps, successive casting was used until the desired crystal loading of 1.2 mg cm^{-2} for TCNQ and 1 mg cm^{-2} for TTF was achieved. The polymer with CTC (TCNQ and THF) was then dried for 24 h under ambient conditions.

The third step was to spread an excess amount of GOx (20 mg mL^{-1} in phosphate buffer, pH 7) over the CTC electrode. Then the electrode was kept for 90 min at 4 ^{0}C, followed by removal of the excess amount of enzyme solution and drying the film at room temperature for 30 min.

The fourth step was spreading of 40 μL cm^{-2} of gelatin (2.5 % in water, incubated for 30 min at 30 ^{0}C before use) over the CTC/GOx structure, followed by drying for 30 min.

Finally, the electrode was dipped into a glutaraldehyde solution (5 % in water) for 60 s, washed with plenty of water and dried at room temperature for 30 min. Schematic presentation of the polypyrrole/CTC/enzyme electrode is shown in Fig. 1c.

Results and discussion

Electrode characterization

The electrode characterization was performed by SEM and by cyclic voltammetry in the buffer electrolyte.

SEM

SEM images of the gold electrode before and after amalgamation are shown in Fig. 2. The surface before amalgamation (Fig. 2a) was subjected to electrochemical polishing and flame annealing, which resulted in low surface roughness (ca. 1.2 estimated by calculating the charge associated with gold oxide reduction peak in 0.1 M H_2SO_4[30]), which is documented in Fig. 2a. After amalgamation, surface roughness increased significantly (it was usually 25 ± 5, which corresponded to 10 s contact time with Hg) and the formation of very

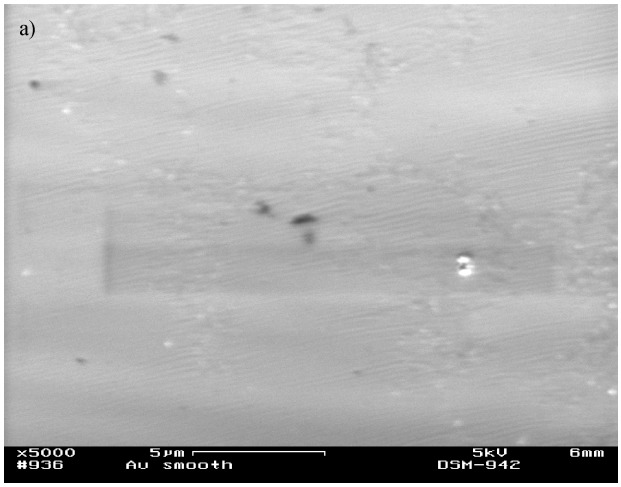

F i g . 2 – *SEM images of the gold surface a) after flame annealing and b) after amalgamation*

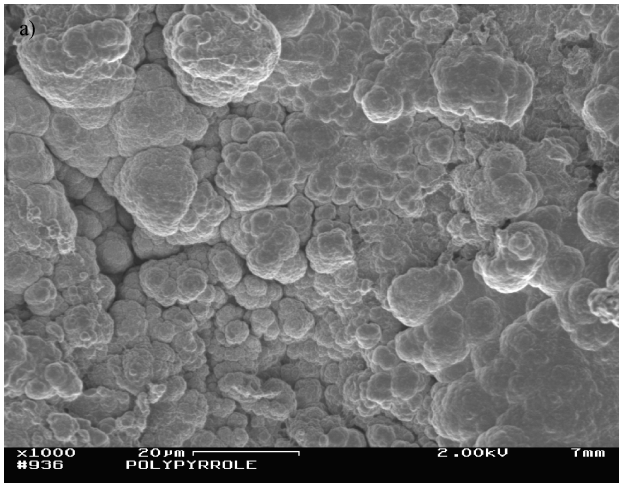

F i g . 3 – *SEM images of the a) polypyrrole layer and b) polypyrrole/CTC/enzyme electrode*

rough surface may clearly be seen in Fig. 2b. The SEM micrograph of gold/SAM shows no significant difference to rough gold surface (not shown here).

In Fig. 3, the SEM images of the polypyrrole layer grown on stainless steel (Fig. 3a) and the polymer/CTC assembly (Fig. 3b) are shown. As obvious from Fig. 3a, the polymer film also had a very high surface roughness. According to the literature,[31] the morphology of the polymer surface may be influenced by the concentration of monomer in the solution, by the dopant anion, by the electropolymerisation conditions (galvanostatic, potentiostatic or potential cycling), etc. In this case, PVS was used as a dopant anion since it is known that larger polyanions provide films with better electrical and mechanical properties.[32] The CTC/polymer surface shown in Fig. 3b also had rough surface structure. The tree-like structure described in the literature[26] could not be observed and instead needle-shaped crystals of CTC lying on the surface of the TCNQ crystals are visible. Possible reasons are the higher roughness of the underlying polypyrrole film and the higher CTC loading in the present study.

Electrochemical characterization

Electrochemical characterization was performed in buffer solution at room temperature and 37 ^{0}C. In Fig. 4a the cyclic voltammograms of freshly prepared rough gold surface (dashed line), rough gold after SAM modification (full grey line) and rough gold after electrochemical activation (full black line) are shown. The freshly prepared rough gold surface had two major redox peaks, which appeared at approx. –0.19 V and 0.17 V. As it was discussed in our recent paper,[10] these voltammetric features may be assigned to OH adsorption on different single crystal domains of the

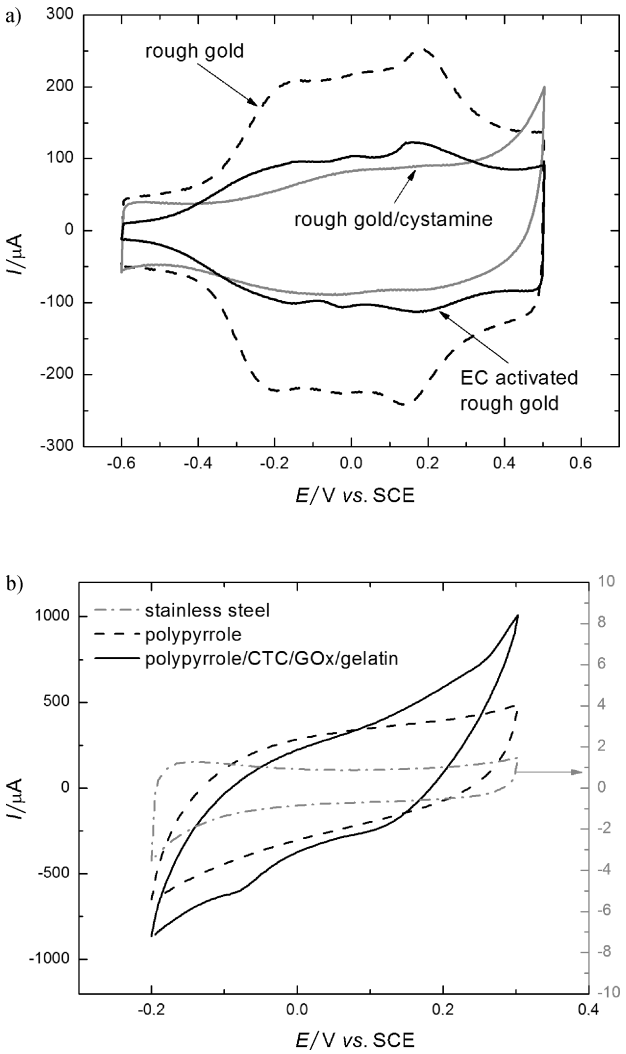

F i g . 4 – *Cyclic voltammograms showing the preconditioning and modification of a) rough gold and b) the enzymatic electrode. Conditions: 0.1 M phosphate buffer, pH 7.2; temperature: room except for the EC activated surface and the enzyme electrode (37 ^{0}C); sweep rate: a) 100 mV s^{-1} and b) 50 mV s^{-1}.*

polycrystalline structure.[7] This surface was further modified by SAM at room temperature, which resulted in rough gold/cystamine surface. The formation of SAM causes the suppression of gold voltammetric features, but a complete monolayer was not formed (the SAM surface coverage was estimated to be 0.6). Freshly prepared rough gold surface exhibits high activity for glucose oxidation at room temperature. However, at 37 ^{0}C it turns into inactive form[10] and this transformation occurs within several minutes. To prevent this inactivation, before glucose oxidation, rough gold was subjected to electrochemical preconditioning (potential cycling in the potential range –1 V to 1.3 V at pH 7.2). As may be seen in Fig. 4a, the voltammetric features of the EC activated rough gold surface were similar to rough gold surface, and only a decrease in surface area was observed.

The formation of polypyrrole/CTC/GOx was monitored by cyclic voltammetry (Fig. 4b). The stainless steel surface was conditioned by mechanical polishing. As may be seen, the surface was relatively smooth (current values were in the range ± 2 μA) and relatively featureless. The formed polypyrrole layer had a high surface area, which could be observed by the increase in the capacitive currents (more than 100 times in comparison to stainless steel substrate), which was already observed in the SEM micrograph (Fig. 3a). As discussed, polypyrrole film was formed galvanostatically in the presence of PVS as a dopant and the thickness of the film was estimated to be 15 μm (based on the charge passed during the electropolymerisation[33]). Further modification of the polymer layer with CTC, GOx and gelatine produced enzyme electrode (Fig. 4b). The voltammetric features of the enzymatic electrode were in accordance with literature results.[23] Similar as other studies,[23] the cathodic peak at about –0.05 V and the onset of anodic peak at approximately 0.2 V were observed. The high capacitive currents indicate again high surface roughness, as already observed in SEM micrographs.

Influence of electrode rotation rate

The influence of mass transport conditions was investigated by changing the electrode rotation rate in the range from 400 – 3600 rpm. As may be seen in Fig. 5, the increase in rotation rate causes an increase of the currents for all three investigated systems (for the sake of clarity only forward scans are shown). The increase of currents does not follow the typical Levich's equation for diffusion limiting current (see Fig. 6 results for rough gold and gold/SAM electrodes). Experimental points show strong deviation from Levich's equation and this kind of behavior is characteristic for systems with reaction limiting current. In this case, the currents in the limiting current region could be calculated using following equation:

$$\frac{1}{I} = \frac{1}{I_{\mathrm{L}}} + \frac{1}{I_{\mathrm{kin}}} \qquad (1)$$

where I_{L} is diffusion limiting current calculated using Levich's equation and I_{kin} is reaction limiting current, which does not depend on the mass transfer conditions. The reaction limiting current for rough gold electrode (second peak at 0.23 V) was estimated to be 481 μA, while in the case of gold/SAM electrode the estimated value (also second peak at 0.25 V) was 206 μA. As may be seen in Fig. 6, the

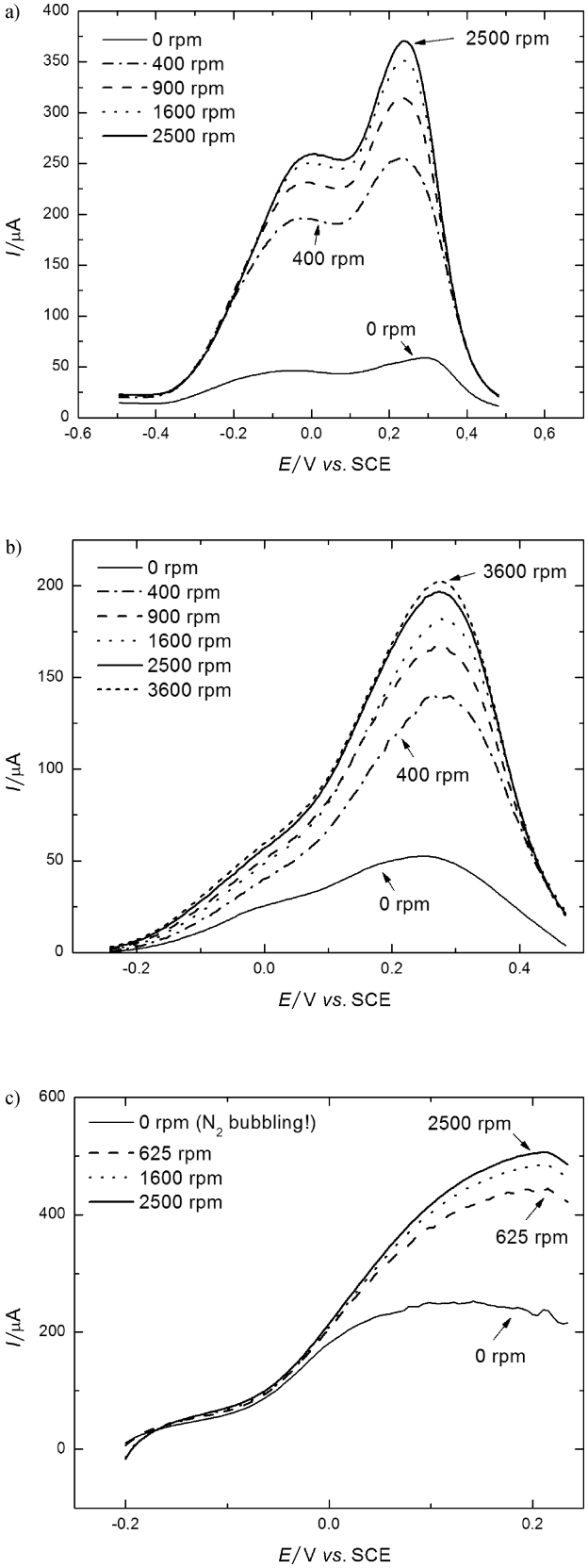

Fig. 5 – *Cyclic voltammograms (only forward scans) in presence of glucose at different rotation rates of a) rough gold, b) rough gold/cystamine and c) polypyrrole/CTC/enzyme electrodes. Conditions: 5 mM glucose in 0.1 M phosphate buffer, pH 7.2; temperature: 37 ^{0}C; sweep rate: 20 mV s^{-1}. Data corrected for background currents.*

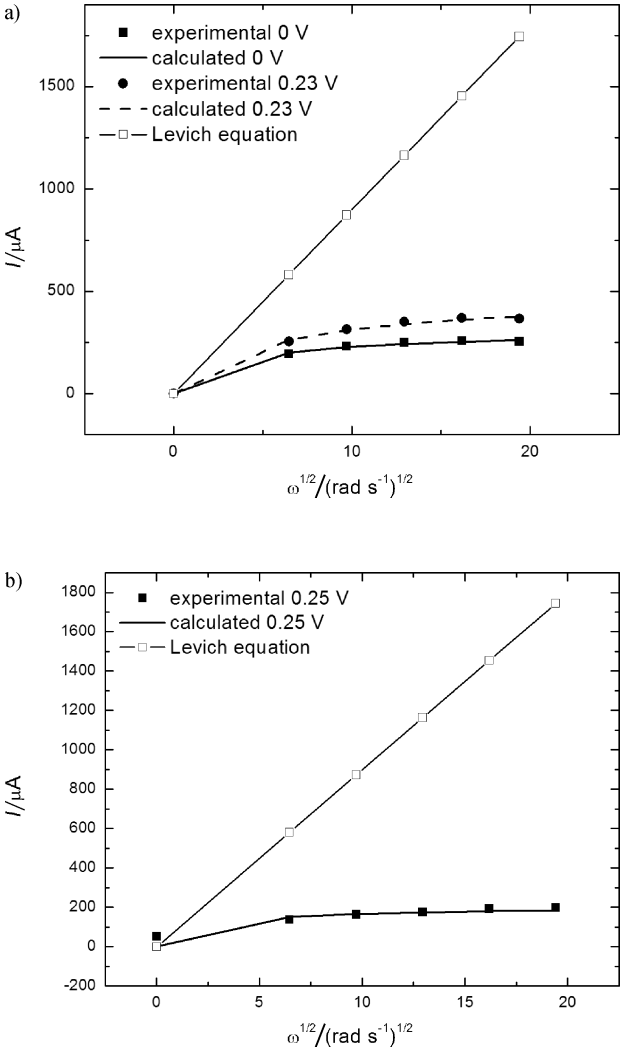

Fig. 6 – *Levich plots of a) rough gold and b) rough gold/cystamine. Data derived from Fig. 5.*

calculated current values (eq. 1) are in a good agreement with the experimental data.

It is known that the reaction limiting currents are proportional to real surface area of the electrode, which means that the ratio between reaction limiting current in the presence of SAM (gold/SAM) and absence of SAM (EC activated rough gold) can give the part of the surface which is not covered by SAM. The value of about 0.43 was obtained. This is in good accordance with previously determined surface coverage by SAM (0.6 which corresponds to 0.4 for the free surface).

Influence of glucose concentration

The influence of glucose concentration was studied in the concentration range 1 – 50 mM in phosphate buffer at 37 ^{0}C.

The polarization curves of EC activated rough gold electrode at different glucose concentrations

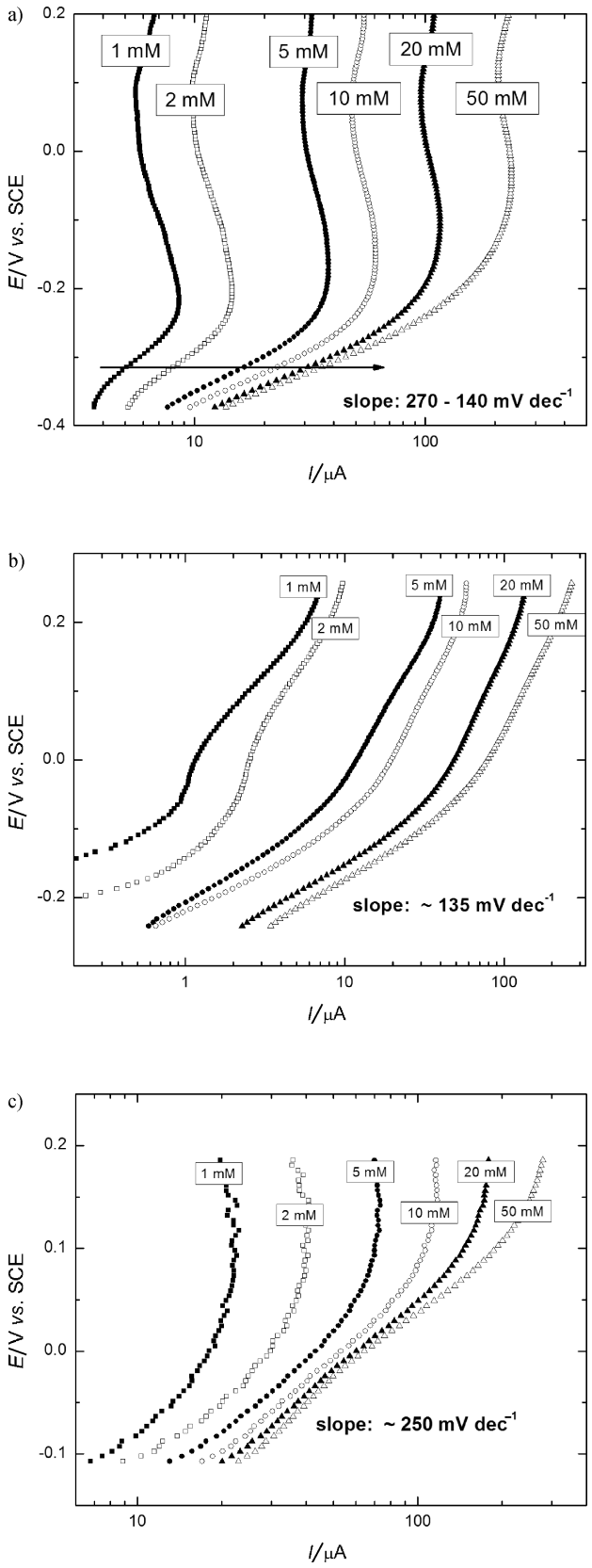

F i g . 7 – *Tafel plots in presence of different glucose concentrations of a) rough gold, b) rough gold/cystamine and c) polypyrrole/CTC/enzyme electrodes. Conditions: 1–50 mM glucose in 0.1 M phosphate buffer, pH 7.2; temperature: 37 ^{0}C; sweep rate: 5 mV s^{-1}; Rotation rate: a) and b) 0 rpm, c) 625 rpm. Data corrected for background currents.*

are shown in Fig. 7a. As previously discussed, due to the fast loss of activity of rough gold, the surface was electrochemically activated by potential cycling in a broad potential window before every measurement. Two separate potential regions can be seen in Fig. 7a. In the first region (ca. –0.4 to –0.25 V) the slope of the semi-logarithmic plot (E vs. log I) is lower and it decreases with the increase in concentration (from 270 mV dec^{-1} at 1 mM to 140 mV dec^{-1} at 50 mM). In this region, the reaction rate depends on potential and shall further herein be referred to as an "activation" controlled region. In the second potential region (–0.2 to 0.2 V), the current remains almost constant with increase in potential i.e. the slope is infinite (further referred to as a limiting current region). As it was already discussed the limiting current is probably mixed reaction-diffusion limited current. Two different regions can also be observed in the corresponding figures for gold/SAM and enzymatic electrode (Fig. 7b and c). In the case of gold/SAM electrode (Fig. 7b), the activation control region shifted to more positive potential values (in comparison to EC activated rough gold) ca. from –0.15 to 0.1 V and the slope value did not change with glucose concentration (ca. 135 mV dec^{-1}). In the case of enzymatic electrode (Fig. 7c), the "low" slope region was in the potential range from –0.1 to 0 V and the slope value was ca. 250 mV dec^{-1}.

In order to obtain a formal reaction order with respect to glucose, the glucose oxidation rates at constant potentials were plotted as a function of the glucose concentrations in logarithmic coordinates for the different catalysts (Fig. 8). As may be seen in Fig. 8a, for the EC activated gold the reaction order with respect to glucose in the activation controlled region (–0.4 to –0.35 V) changed from about 0.5 (0.7) at low concentrations to 0 at higher concentrations, while in the limiting current region (–0.2 to 0.2 V) the reaction order was constant and equal to 0.9. In the case of gold/SAM the reaction order remained unchanged in different potential regions and equaled 1 (Fig. 8b). The enzymatic electrode behaved similar to EC activated rough gold regarding glucose reaction order and in the activation slope region the reaction order changed from 0.4 at low concentrations to 0 at high concentrations, while in the limiting current region it remained constant and equaled 0.7 (Fig. 8c).

To summarize, all investigated electrodes had activation and limiting current regions. The activation controlled region is usually related to dominant electrochemical control of the process which leads to typical slope values of up to 120 mV dec^{-1} (123 mV dec^{-1} at 37 ^{0}C). The slope values observed in this study are much higher (270–140 mV dec^{-1},

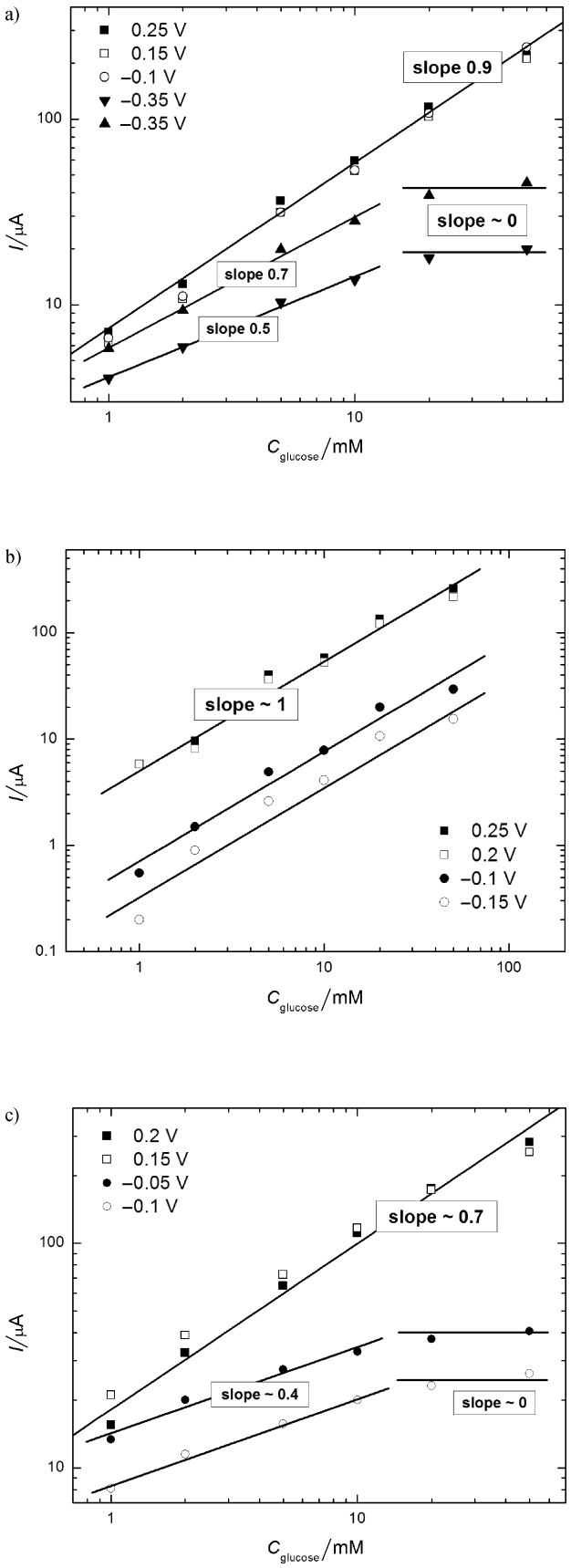

Fig. 8 – *Glucose oxidation currents at constant potentials versus the glucose concentration of a) rough gold, b) rough gold/cystamine and c) polypyrrole/CTC/enzyme electrodes. Data derived from Fig. 7.*

250 mV dec^{-1} for EC activated gold and enzymatic electrode respectively). This indicates that the rate determining step (r.d.s) is not a single electrochemical step, but more likely the combination of two steps (one electrochemical and one chemical). A similar feature was observed in the case of methanol oxidation on PtRu catalyst, where the reaction in the activation controlled region was controlled by two steps: slow methanol adsorption (chemical reaction) and surface reaction between adsorbed intermediate and OH on the surface (electrochemical reaction).[34] In addition, different reaction orders were obtained in different potential regions.

In the case of gold/SAM electrode, the Tafel slope was 135 mV dec^{-1} and the reaction order was 1, which is similar to kinetic parameters determined for Au(111) single crystal surface determined in previous studies.[7] In our previous paper, it was discussed that the gold/SAM surface had surface domains corresponding to Au(111) single crystal domains, which was in accordance with cyclic voltammetry characterization, SAM desorption and onset and peak potential of glucose oxidation peak.[10] These additional kinetic parameters are supporting evidence for the formation of Au(111) single crystal domains on rough gold/SAM surface.

Influence of oxygen

It was already mentioned in the introduction that the catalyst for glucose oxidation that can tolerate the fuel and oxidant in the same solution has an advantage, since it enables a simpler fuel-cell design (membraneless fuel cell). In Fig. 9, cyclic voltammograms showing the activity for glucose oxidation of the two metal catalysts (Figs. 9a, b) and the biocatalyst (Fig. 9c) in the absence and presence of oxygen are shown. It can be seen that the enzymatic catalyst is much more oxygen-tolerant than the two metal catalysts. This is in accordance with some literature results,[26] where oxygen also had a minor influence due to very fast electron transfer between the enzyme and the CTC. The use of two metal catalysts in the presence of oxygen is possible only in the potential region more positive than 0.1 V. This will however increase the overpotential for glucose oxidation and decrease the expected fuel cell performance.

Stability

The stability of the three electrodes was tested by polarizing them for half an hour in the presence of 5 mM of glucose in a phosphate buffer solution, oxygen free atmosphere, and at rotation rate of

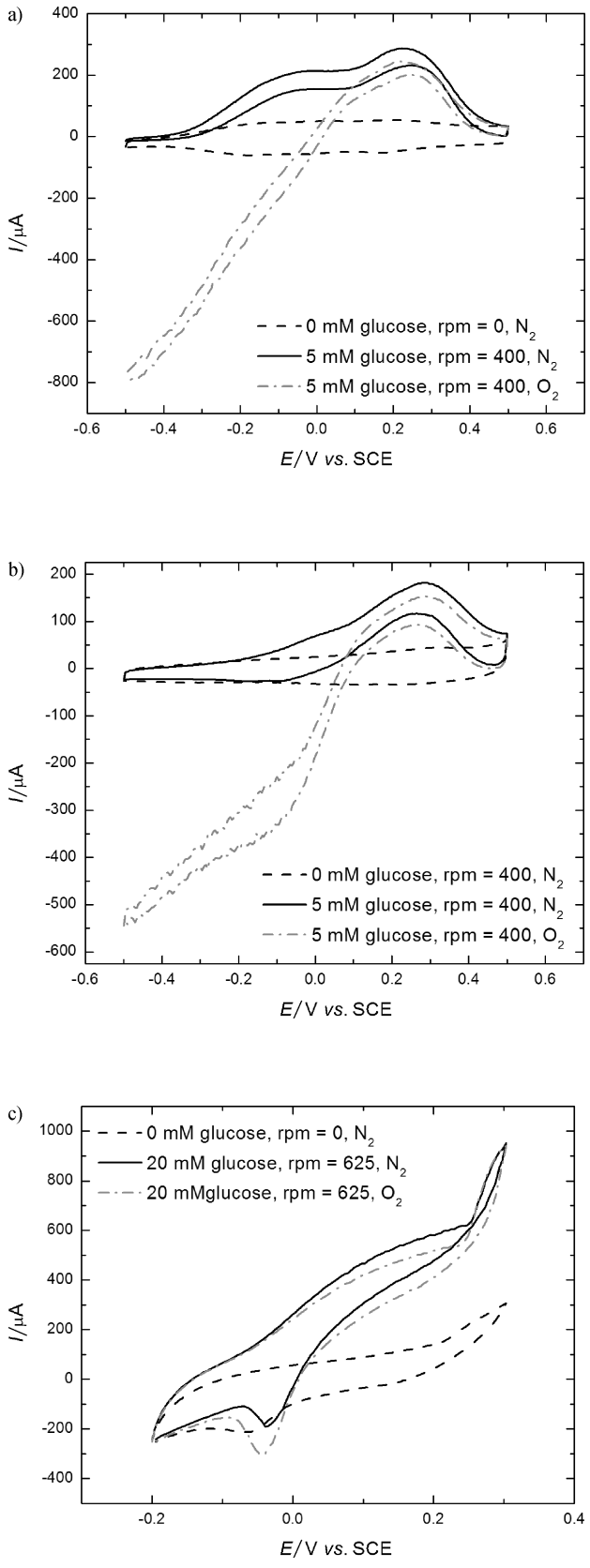

F i g . 9 – *Cyclic voltammograms in absence (N_2 atmosphere) and presence of glucose (N_2 and O_2 atmosphere) at different rotation rates of a) rough gold, b) rough gold/cystamine and c) polypyrrole/CTC/enzyme electrodes. Conditions: 0–20 mM glucose in 0.1 M phosphate buffer, pH 7.2; temperature: 37 ^{0}C; sweep rate: a) and b) 50 mV s^{-1}, c) 5 mV s^{-1}.*

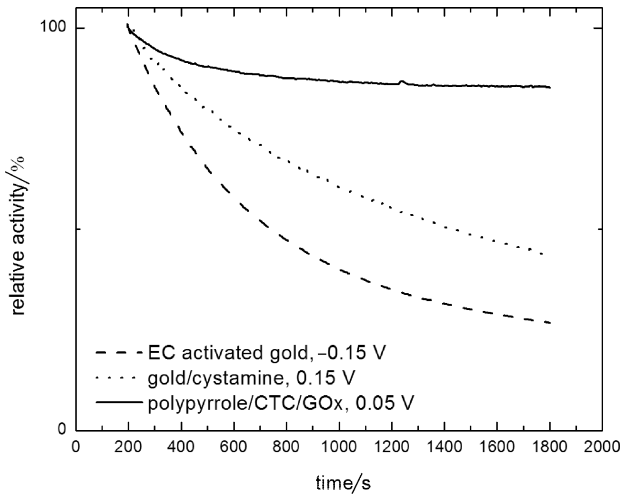

F i g . 1 0 – *Chronoamperograms at different potentials of the different electrodes. Conditions: 5 mM glucose in 0.1 M phosphate buffer, pH 7.2; temperature: 37 ^{0}C; rotation rate: 400 rpm; N_2 atmosphere. Current after 200 s taken as a reference (100 %).*

400 rpm. The electrodes were polarized at different potential values, which corresponded to current responses in the respective limiting current regions. Since the enzymatic electrode had very high capacitive currents due to the underlying polymer layer, the current after 200 s was used as a referent value (corresponds to 100 % of activity). As obvious from Fig. 10, the enzymatic electrode showed a very stable response (it preserved 85 % of its initial activity after 30 min). The metal electrodes were less stable and preserved only 43 % and 27 % (gold/SAM and rough gold, respectively) of initial activity. The extreme instability of the EC activated gold excludes its application as an anode in a glucose-air fuel cell, although it has a quite negative oxidation onset (low overpotential for glucose oxidation).

Conclusions

The kinetics of glucose oxidation on two metal catalysts and one biocatalyst was investigated. According to the determined kinetic parameters, the reaction mechanisms for glucose oxidation on rough gold and enzymatic electrode are complicated (no single reaction step could be assigned as r.d.s. and the reaction orders had different values in different potential regions). In the case of gold/SAM electrode, the determined kinetic parameters were in good agreement with values obtained for Au(111) single crystal plane. This is further evidence for the presence of Au(111) domains on rough gold modified by SAM. Regarding onset potential for glucose oxidation, metal electrodes per-

formed better but they exhibited lower stability and lower O_2 tolerance. Further modeling work is needed to gain a better understanding of the kinetics of glucose oxidation on these surfaces. The enzymatic electrode showed good performance but it still needs some optimization.

References

1. *Wang, J.,* Chem. Rev. **108** (2008) 814.
2. *Moehlenbrock, M. J., Minteer, S. D.,* Chem. Soc. Rev. **37** (2008) 1188.
3. *Park, S., Boo, H., Chung, T. D.,* Anal. Chim. Acta **556** (2006) 46.
4. *Barton, S. C., Gallaway, J., Atanassov, P.,* Chem. Rev. **104** (2004) 4867.
5. *Tominaga, M., Shimazoe, T., Nagashima, M., Taniguchi, I.,* Electrochem. Comm. **7** (2005) 189.
6. *Hsiao, M. W., Adžić, R. R., Yeager, E. B.,* Electrochim. Acta **37** (1992) 357.
7. *Hsiao, M. W., Adžić, R. R., Yeager, E. B.,* J. Electrochem. Soc. **143** (1996) 759.
8. *Cho, S., Shin, H., Kang, C.,* Electrochim. Acta **51** (2006) 3781.
9. *Cho, S., Kang, C.,* Electroanalysis **19** (2007) 2315.
10. *Ivanov, I., Vidaković, T. R., Sundmacher, K.,* Electrochem. Comm. **10** (2008) 1307.
11. *Martins, A., Ferreira, V., Queirós, A., Aroso, I., Silva, F., Feliu, J.,* Electrochem. Comm. **5** (2003) 741.
12. *Makovos, E. B., Liu, C. C.,* Bioelectroch. Bioener. **15** (1986) 157.
13. *Aoun, S. B., Dursun, Z., Koga, T., Bang, G. S., Sotomura, T., Taniguchi, I.,* J. Electroanal. Chem. **567** (2004) 175.
14. *Jin, C., Taniguchi, I.,* Materials Letters **61** (2007) 2365.
15. *Habrioux, A., Sibert, E., Servat, K., Vogel, W., Kokoh, K. B., Alonso-Vante, N.,* J. Phys. Chem. B **111** (2007) 10329.
16. *El-Deab, M. S., Arihara, K., Ohsaka, T.,* J. Electrochem. Soc. **151** (2004) E213.
17. *Wilson, R., Turner, A. P. F.,* Biosens. Bioelectron. **7** (1992) 165.
18. *Degani, Y., Heller, A.,* J. Am. Chem. Soc. **111** (1989) 2357.
19. *Sun, Y., Sun, J., Zhang, X., Sun, C., Wang, Y., Shen, J.,* Thin Solid Films **327–329** (1998) 730.
20. *Reiter, S., Habermüller, K., Schuhmann, W.,* Sens. Actuat. B **79** (2001) 150.
21. *Barriere, F., Kavanagh, P., Leech, D.,* Electrochim. Acta **51** (2006) 5187.
22. *Čenas, N. K., Kulys, J. J.,* Bioelectroch. Bioener. **8** (1981) 103.
23. *Kulys, J. J.,* Biosensors **2** (1986) 3.
24. *Cano, M., Ávila, J. L., Mayén, M., Mena, M. L., Pingarrón, J., Rodríguez-Amaro, R.,* J. Electroanal. Chem. **615** (2008) 69.
25. *Albery, W. J., Bartlett, P. N., Craston, D. H.,* J. Electroanal. Chem. **194** (1985) 223.
26. *Khan, G. F., Ohwa, M., Wernet, W.,* Anal. Chem. **68** (1996) 2939.
27. *Khan, G. F.,* Sensors and Actuators B **35–36** (1996) 484.
28. *Pauliukaite, R., Malinauskas, A., Zhylyak, G., Spichiger-Keller, U. E.,* Electroanalysis **19** (2007) 2491.
29. *Engelsmann, K., Loreny, W. J.,* J. Electroanal. Chem. **114** (1980) 1.
30. *Tremiliosi-Filho, G., Dall'Antonia, L. H., Jerkiewicz, G.,* J. Electroanal. Chem. **422** (1997) 149.
31. *Vernitskaya, T. V., Efimov, O. N.,* Russ. Chem. Rev. **66** (5) (1997) 443.
32. *Warren, L. F., Anderson, D. P.,* J. Electrochem. Soc. **134** (1987) 101.
33. *Inganäs, O., Erlandsson, R., Nylander, C., Lundström, I.,* J. Phys. Chem. Solids **45** (1984) 427.
34. *Vidaković, T., Christov, M., Sundmacher, K.,* J. Electroanal. Chem. **580** (2005) 105.